

Two Copper-Rich Open-Framework Chalcogenides Built from Unusual $[\text{Cu}_5(\text{Sn}_x\text{M}_{1-x})\text{Se}_{10}]$ Cluster and $[(\text{Sn}_x\text{M}_{1-x})_2\text{Se}_6]$ Dimeric Linker (M = In and Ga)

Bing Han,^{†,¶} Jing Wang,^{‡,¶} Yong Liu,[†] Xiang Wang,[†] Chaozhuang Xue,[†] Jing Lv,[†] Zhou Wu,[†] Rui Zhou,[†] Dingguo Xu,^{*,‡} Dong-Sheng Li,[§] and Tao Wu^{*,†}

[†] College of Chemistry, Chemical Engineering and Materials Science, Soochow University, Suzhou, Jiangsu 215123, China

[‡] College of Chemistry, Sichuan University, Chengdu 610064, China

[§] College of Materials and Chemical Engineering, Hubei Provincial Collaborative Innovation Center for New Energy Microgrid, Key Laboratory of Inorganic Nonmetallic Crystalline and Energy Conversion Materials, China Three Gorges University, Yichang, Hubei 443002, China

[¶] These authors contributed equally.

E-mail: wutao@suda.edu.cn; dgxu@scu.edu.cn

Experimental Section

Materials. Copper (Cu, 99.9%, powder), indium powder (In, 99.99%, powder), gallium metal (Ga, AP, bulk), tin (Sn, 99.9%, powder), selenium (Se, 99.9%, powder), 1,5-diazabicyclo[4.3.0]non-5-ene (DBN, $\geq 98\%$, liquid), and deionized water. All the reagents and solvents used were commercially supplied without further purification. (Caution: the heated autoclaves should be operated when they are completely cooled to room temperature.)

Synthesis of COC-8-In. Copper iodide (90 mg, 0.469 mmol), indium powder (114 mg, 1.0 mmol), Sn (90 mg, 0.968 mmol), selenium powder (197 mg, 2.495 mmol) were mixed with 1,5-diazabicyclo[4.3.0]non-5-ene (DBN, 4 mL) and deionized water (H₂O, 1 mL) in a 23-mL Teflon-lined stainless steel autoclave and stirred for half an hour. The vessel was then sealed and heated at 180 °C for 7 days, then the autoclave was cooled to room temperature. Red rhombus-like crystals were obtained. The raw products were washed three times by ethanol and filtered off, and further purified by hand with a yield of 80 mg.

Synthesis of COC-8-Ga. Copper iodide (90 mg, 0.469 mmol), gallium metal (45 mg, 0.643 mmol), Sn (90 mg, 0.968 mmol), selenium powder (185 mg, 2.342 mmol) were mixed with 1,5-diazabicyclo[4.3.0]non-5-ene (DBN, 4 mL) and deionized water (H₂O, 1 mL) in a 23-mL Teflon-lined stainless steel autoclave and stirred for half an hour. The vessel was then sealed and heated at 190 °C for 7 days, then the autoclave was cooled to room temperature. Red rhombus-like crystals were obtained. The raw products were washed three times by ethanol and filtered off, and further purified by hand with a yield of 50 mg.

Single Crystal X-ray Diffraction (SCXRD). Single-crystal X-ray diffraction measurements were performed on Photon II CPAD diffractometer with nitrogen-flow temperature controlled using graphite-monochromated Mo-K α ($\lambda = 0.71073 \text{ \AA}$) radiation at 120 K. The structure was solved by direct method using SHELXS-97 and the refinements against all reflections of the compound were performed using

SHELXL-97.

Powder X-ray Diffraction (PXRD). PXRD data were collected on a desktop diffractometer (D2 PHASER, Bruker, Germany) using Cu-K α ($\lambda = 1.54184 \text{ \AA}$) radiation operated at 30 kV and 10 mA. The samples were ground into fine powders for several minutes before the test.

Elemental Analysis. Energy dispersive spectroscopy (EDS) analysis was performed on scanning electron microscope (SEM) equipped with energy dispersive spectroscopy detector. An accelerating voltage of 25 kV and 40 s accumulation time were applied. EDS results clearly confirmed the presence of Cu, In, Ga and Se elements. Elemental analysis of C, H, and N was performed on VARIDEL III elemental analyzer.

Thermogravimetric Analysis (TGA). A Shimadzu TGA-50 thermal analyzer was used to measure the TG curve by heating the sample from room temperature to 800 °C with heating rate of 10 °C/min under N₂ flow.

UV-Vis Absorption. Room-temperature solid-state UV-Vis diffusion reflectance spectra of crystal samples were measured on a SHIMADZU UV-3600 UV-Vis-NIR spectrophotometer coupled with an integrating sphere by using BaSO₄ powder as the reflectance reference. The absorption spectra were calculated from reflectance spectra by using the Kubelka-Munk function: $F(R)=\alpha/S=(1-R)^2/2R$, where R , α , and S are the reflection, the absorption and the scattering coefficient, respectively.

Computational details. The density functional theory (DFT)^{1, 2} calculations were performed by applying the projector-augmented wave (PAW) scheme³ within the Vienna ab initio Simulation Package (VASP)^{4, 5} version 5.4.4. For the geometry optimizations, generalized gradient approximation (GGA) with Perdew–Burke–Ernzerhof (PBE) parameterization^{6, 7} was used as the exchange–correlation functional. While for the density of states (DOS) calculation, the hybrid exchange–correlation functional (HSE06)^{7, 8} was employed in our simulations. The plane-wave energy cutoff was set as 300 eV in all calculations. The energy convergence was set to be

10^{-5} eV.

XPS and AES Measurements. X-ray photoelectron spectroscopy (XPS) and Auger electron spectroscopy (AES) were collected with a Leeman prodigy spectrometer equipped with a monochromatic Al K α X-ray source and a concentric hemispherical analyzer.

Photoelectric Response. The photocurrent experiments were performed on a CHI 760E electrochemistry workstation in standard three-electrode configuration, with the sample coated ITO glass (the effective area is around 1 cm²) as the working electrode, a Pt wire as the auxiliary electrode, and a saturated calomel electrode (SCE) as the reference electrode. The light source is a 150 W high pressure xenon lamp, located 20 cm away from the surface of the ITO electrode. Sodium sulfate aqueous solution (0.5 M, 100 mL) was used as the supporting electrolyte. Typical preparation of film of **COC-8-In** and **COC-8-Ga** on ITO electrode: 5.0 mg of ground **COC-8-In** and **COC-8-Ga** powder was dispersed in 10 mL isopropanol with the presence of 1.0 mg of Mg(NO₃)₂·6H₂O. The sealed mixture suspension was continuously stirred for one day, and then was ultrasonically vibrated for half hour before electrophoretic deposition. The clean and sleek Pt plate electrode was used as anode, and the indium-tin-oxide (ITO) conductive glass as cathode. Constant working voltage was set up to 30 V. The whole electro-deposition process lasted for 30 min. The obtained ITO electrode decorated with **COC-8-In/COC-8-Ga** film on its surface was finally washed with ethanol to remove residual isopropanol and Mg(NO₃)₂ salt left in suspension.

Methylene Blue Photo-degradation Process. The catalytic activities of the as-synthesized samples were evaluated by the degradation reactions of Methylene Blue (MB) dye. The samples were immersed in 20 mL of MB (1.8×10^{-5} mol • L⁻¹) aqueous solution and stirred for 30 min and remained for 60 min before irradiation in the dark to reach the adsorption/desorption equilibrium. During irradiation, 3 mL of suspension was sucked up from the reaction reactor at certain interval times and analyzed on UV-vis spectrophotometer. The degradation efficiency was reported as

C_t/C_0 , where C_t and C_0 main peak of the absorption at each irradiated time interval and equilibrium concentration of MB.

Check CIF results

Due to the low resolution of sulfides, it is difficult to distinguish the positions of trivalent and tetravalent metals in the COC-8 compounds *via* single crystal X-ray diffraction. One of the main reasons is that there is no difference in bond length between these metal sites and selenium atoms. Moreover, COC-8 compounds have 10 Sn sites on each asymmetric unit, so it is difficult to know how In/Ga and Sn share the metal sites. So our solution is to refine it all with Sn atoms and then combine the EDS results to determine the proportion of trivalent and tetravalent metals in the compounds.

COC-8-In (CCDC number: 1911102)

Alert Level A

THETM01_ALERT_3_A The value of $\sin(\theta_{\max})/\lambda$ is less than 0.550

Calculated $\sin(\theta_{\max})/\lambda = 0.4171$

Response: The diffraction capability of open-framework chalcogenide is weak. It's hard to harvest diffraction point at high angle, which results in the resolution of a bit lower 0.83 (Mo-K α).

Alert Level B

PLAT910_ALERT_3_B Missing # of FCF Reflection(s) Below Theta (Min). 17 Note

Response:

These issues of alert level B possibly result from low resolution and some weak diffraction points of the crystal. Other single crystals are also tested for getting better diffraction data, unfortunately, several groups of data show similar crystallographic issues.

COC-8-Ga (CCDC number: 1966355)

Alert Level A

THETM01_ALERT_3_A The value of $\sin(\theta_{\max})/\lambda$ is less than 0.550

Calculated $\sin(\theta_{\max})/\lambda = 0.3587$

Response: The diffraction capability of crystalline chalcogenide framework is usually weak, and it's hard to harvest high-angle diffraction points, which results in low resolution of 0.83 (Mo-K α).

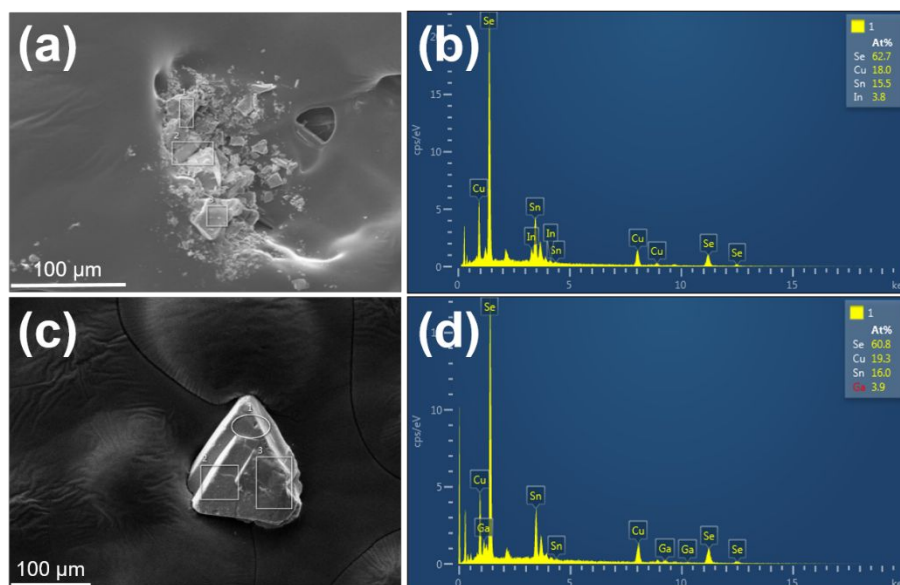


Figure S1. SEM images of as-synthesized **COC-8-In** (a) and **COC-8-Ga** (c), and energy dispersive spectroscopy (EDS) of **COC-8-In** (b) and **COC-8-Ga** (d).

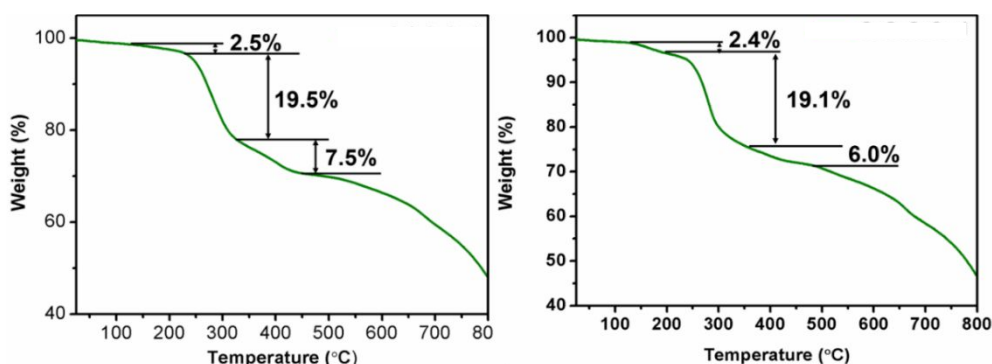


Figure S2. TGA curves of **COC-8-In** (left) and **COC-8-Ga** (right).

Thermogravimetric (TG) analysis of **COC-8-In** shows three decomposition steps. The first weight loss of 2.5 % between 130-230 °C could be the loss of crystal water (*Calcd.* 2.2%). And the abrupt weight loss of around 19.5% occurs between 230-325 °C and 7.5% between 325-450 °C are in good agreement with the removal of DBN (*Calcd.* 19.8%) and hydrogen selenide (7.5%). And for **COC-8-Ga**, the sample goes through the same reaction process as **COC-8-In**. The weight loss about 2.4%, 19.1% and 6.0% are consistent with the calculated values from the SCXRD analysis, corresponding to the removal of crystal water (*Calcd.* 2.2%), DBN (*Calcd.* 20.2%) and hydrogen selenide, respectively.

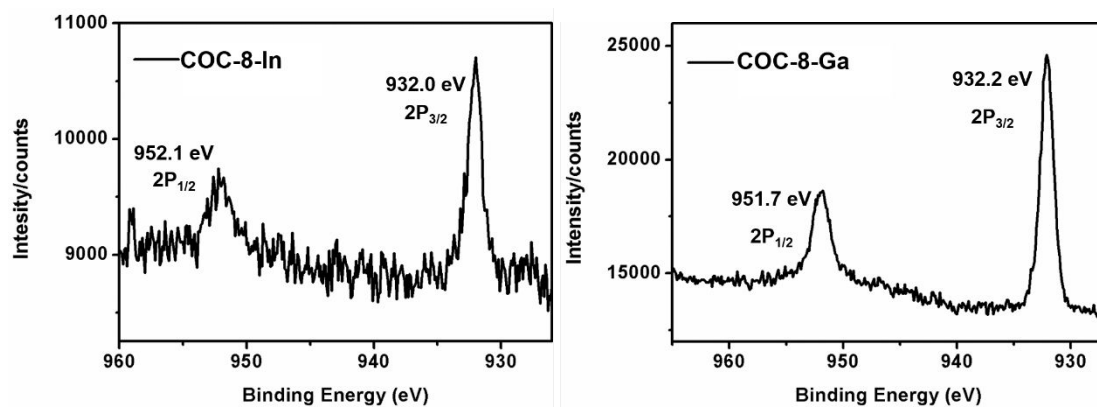


Figure S3. The Cu XPS peaks of **COC-8-In** (left) and **COC-8-Ga** (right).

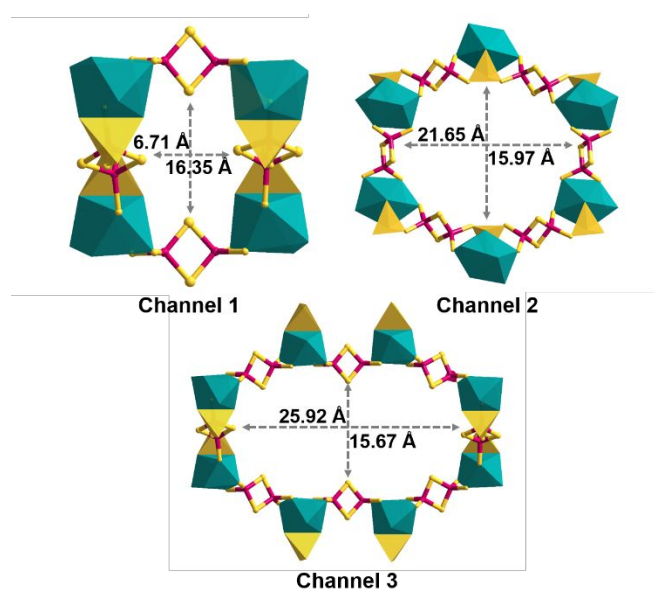


Figure S4. Channels viewed along axis in the as-synthesized **COC-8**. The resulting frameworks exhibit three kinds of 3D channels.

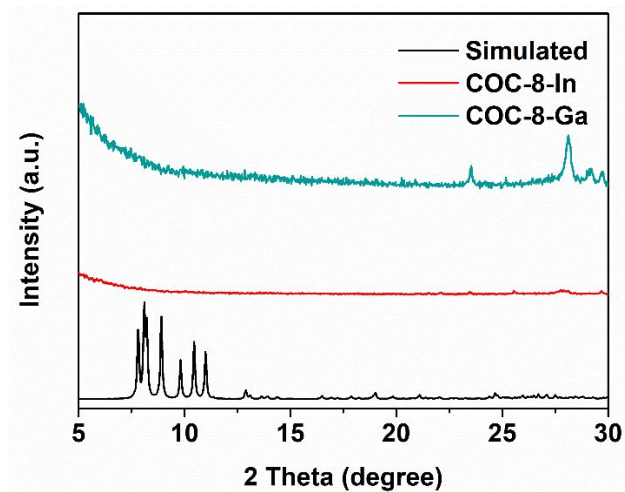


Figure S5. The PXRD patterns of **COC-8-In/Ga** after the treatment of 1 M CsCl aqueous at 85 °C for 24h.

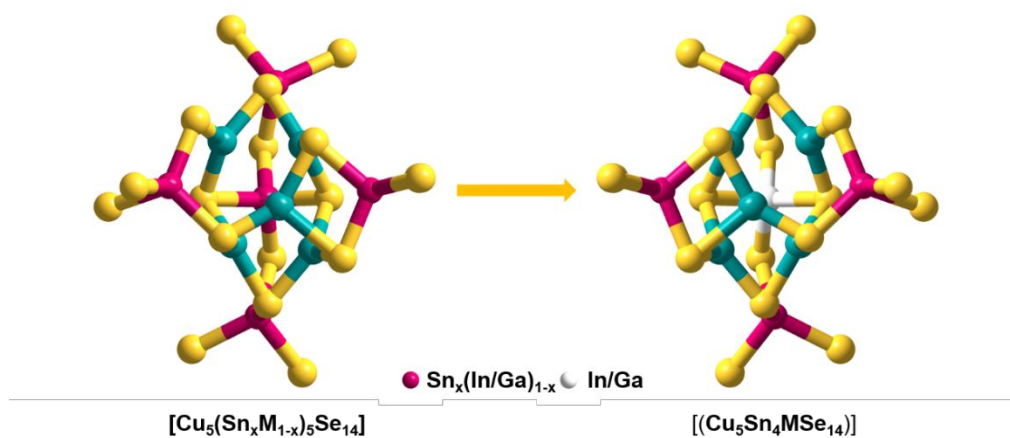


Figure S6. Crystal structure model constructed for theoretical calculation.

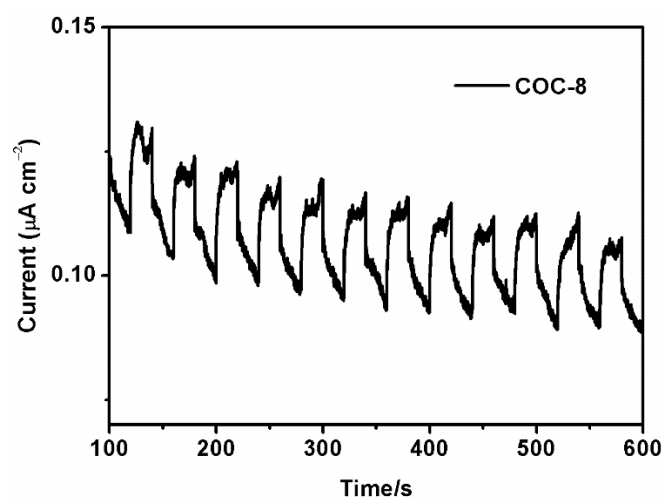


Fig. S7. Zero-bias photocurrent response of the **COC/FTO** electrode under visible light irradiation.

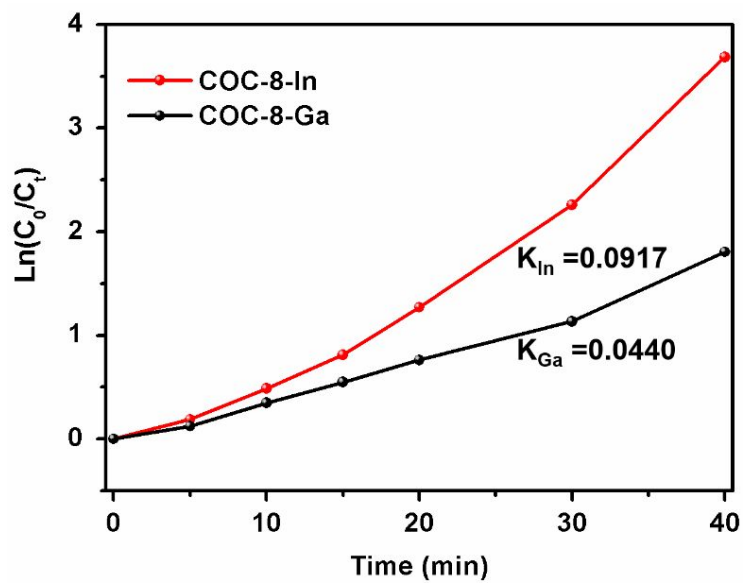


Figure S8. The calculated degradation rate of MB over COC-8.

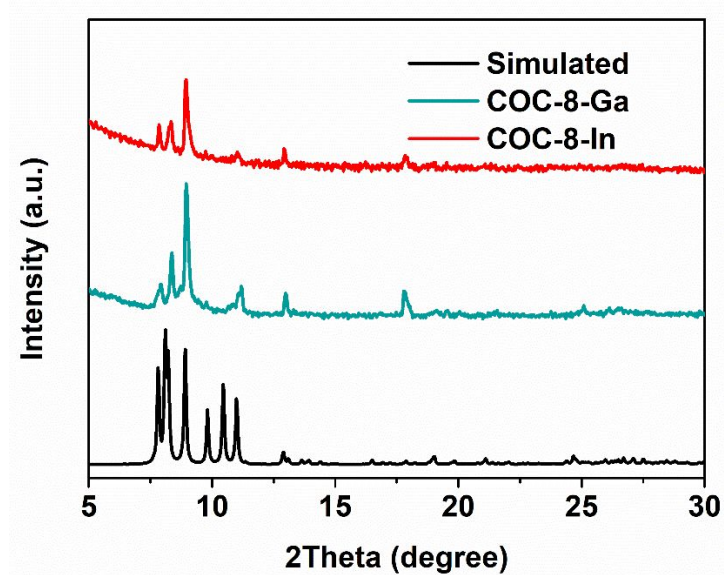


Figure S9. The XRD patterns after photocatalysis dye degradation of COC-8.

Table S1. Summary on the ratio of copper to the other metals in *Tn*-cluster-based chalcogenides and typical copper-rich chalcogenides (**COCs**).

Code	Framework Formula	SBU	Ratio of Cu/A
ISC-10 ⁹	[CuCd ₆ In ₂₈ S ₅₂ (H ₂ O) ₄]	T5	0.03
OCF-40 ¹⁰	[Cu ₂ Ga ₁₆ Sn ₂ Se ₃₃]	T4	0.11
TMA-CuGS-2 ¹¹	[(Cu _{0.44} Ge _{0.56} S _{2.23}) ₄ (Ge ₄ S ₈) ₃]	T2	0.12
UCR-17 ¹²	[Cu ₅ In ₃₀ S ₅₄]	T5	0.17
CIS-11-CuInS ¹³	[Cu ₇ In ₂₈ S ₅₃]	T5	0.25
TEA-CuGS-SBI ¹⁴	[CuGe ₂ S ₅]	T2	0.50
COC-8-In	[Cu ₅ Sn ₄ InSe ₁₄]	[Cu ₅ Sn ₄ InSe ₁₄]	1.00
COC-8-Ga	[Cu ₅ Sn ₄ GaSe ₁₄]	[Cu ₅ Sn ₄ GaSe ₁₄]	1.00
Compound 1 ¹⁵	[Cu ₈ Sn ₆ Se ₁₉]	[Cu ₈ Se ₁₃]	1.33
GeCuS-1 ¹⁶	[Cu ₈ Ge ₅ S ₁₆]	[Cu ₈ S ₁₂]	1.60
Compound 2 ¹⁷	[Cu ₇ Sn ₄ S ₁₂]	[Cu ₈ S ₁₂]	1.75
Compound 3 ¹⁸	[Cu ₈ Ge ₄ S ₁₄]	[Cu ₈ S ₁₂]	2.00
Compound 4 ¹⁹	[Cu ₈ Sn ₃ S ₁₂]	[Cu ₈ S ₁₂]	2.67

Table S2. Elementary analysis result of C, H and N for COC-8.

		C	H	N
COC-8-In	Calculated (wt.%)	13.34	2.43	4.45
	Found (wt.%)	13.44	2.42	4.45
COC-8-Ga	Calculated (wt.%)	13.58	2.47	4.52
	Found (wt.%)	13.83	2.19	4.78

Table S3. The table of the EDS analysis of **COC-8-In** and **COC-8-Ga**.

Sample	Sn/In(Ga)			Average
	1	2	3	
COC-8-In	4.18	3.88	4.07	4.04
	3.95	4.10	4.05	
COC-8-Ga	3.95	4.10	4.05	4.03
	4.18	3.88	4.07	

Table S4. The crystal data and refinement details of **COC-8**.

Compounds	COC-8-In	COC-8-Ga
Crystal system	monoclinic	monoclinic
Space group	<i>P2/c</i>	<i>P2/c</i>
<i>Z</i>	4	4
<i>T/K</i>	120	120
<i>a</i> (Å)	40.055 (2)	40.019 (4)
<i>b</i> (Å)	13.7354 (8)	13.6291 (15)
<i>c</i> (Å)	21.6946 (13)	21.235 (2)
α (deg.)	90	90
β (deg.)	97.034 (2)	97.537 (2)
γ (deg.)	90	90
<i>V</i> (Å ³)	11845.9 (12)	11482 (2)
<i>F</i> (000)	6968	6968
<i>D</i> (g cm ⁻³)	2.262	2.333
Collected reflections	55446	52338
Independent reflections	7210	4443
GOF on <i>F</i> ²	1.110	1.070
<i>R</i> ₁ , <i>wR</i> ₂ (<i>I</i> > 2σ(<i>I</i>))	0.0636, 0.1440	0.0782, 0.2247
<i>R</i> ₁ , <i>wR</i> ₂ (all data)	0.0675, 0.1461	0.0831, 0.2365

References:

1. Hadjisavvas, N.; Theophilou, A. Rigorous formulation of the Kohn and Sham theory. *Phys. Rev. A*. **1984**, *30*, 2183-2186.
2. Kohn, W.; Sham, L. J. Self-Consistent Equations Including Exchange and Correlation Effects. *Phys. Rev.* **1965**, *140*, A1133-A1138.
3. Blöchl, P. E. Projector augmented-wave method. *Phys. Rev.* **1994**, *50*, 17953-17979.
4. Furthmüller, G. K. J. Efficient iterative schemes for ab initio total-energy calculations using a plane-wave basis set. *Phys. Rev. B*. **1996**, *54*, 11169-11186.
5. G, Kresse.; J, Furthmüller. Efficiency of ab-initio total energy calculations for metals and semiconductors using a plane-wave basis set. *Comp. Mater. Sci.* **1996**, *54*, 11169-11186.
6. John P. Perdew, K. B. Matthias Ernzerhof, Generalized Gradient Approximation Made Simple. *Phys. Rev. Lett.* **1996**, *77*, 3865-3868.
7. Krukau, A. V.; Vydrov, O. A.; Izmaylov, A. F.; Scuseria, G. E. Influence of the exchange screening parameter on the performance of screened hybrid functionals. *J. Chem. Phys.* **2006**, *125*, 224106.
8. Heyd, J.; Scuseria, G. E. Efficient hybrid density functional calculations in solids: assessment of the Heyd-Scuseria-Ernzerhof screened Coulomb hybrid functional. *J. Chem. Phys.* **2004**, *121*, 1187-1192.
9. Wu, T.; Zhang, Q.; Hou, Y.; Wang, L.; Mao, C.; Zheng, S. T.; Bu, X.; Feng, P. Monocopper doping in Cd-In-S supertetrahedral nanocluster via two-step strategy and enhanced photoelectric response. *J. Am. Chem. Soc.* **2013**, *135*, 10250-10253.
10. Wu, T.; Wang, L.; Bu, X.; Chau, V.; Feng, P. Largest Molecular Clusters in the Supertetrahedral Tn Series. *J. Am. Chem. Soc.* **2010**, *132*, 10823-10831.
11. Tan, K.; Ko, Y.; Parise, J. B.; Darovsky, A. J. C. o. m. Hydrothermal growth of single crystals of TMA-CuGS-2, $[C_4H_{12}N]_6[(Cu_{0.44}Ge_{0.56}S_{2.23})_4(Ge_4S_8)_3]$ and their characterization using synchrotron/imaging plate data. *Chem. Mater.* **1996**, *8*, 448-453.
12. Bu, X.; Zheng, N.; Li, Y.; Feng, P. Pushing Up the Size Limit of Chalcogenide Supertetrahedral Clusters: Two- and Three-Dimensional Photoluminescent Open Frameworks from $(Cu_5In_{30}S_{54})^{13-}$ Clusters. *J. Am. Chem. Soc.* **2002**, *124*, 12646-12647.
13. Wang, L.; Wu, T.; Zuo, F.; Zhao, X.; Bu, X.; Wu, J.; Feng, P. Assembly of supertetrahedral T5 copper-indium sulfide clusters into a super-supertetrahedron of infinite order. *J. Am. Chem. Soc.* **2010**, *132*, 3283-3285.
14. Tan, K.; Darovsky, A.; Parise, J. B. Synthesis of a novel open-framework sulfide, $CuGe_2S_5(C_2H_5)_4N$, and its structure solution using synchrotron imaging plate data. *J. Am. Chem. Soc.* **1995**, *117*, 7039-7040.
15. Luo, M.; Hu, D.; Yang, H.; Li, D.; Wu, T. PCU-type copper-rich open-framework chalcogenides: pushing up the length limit of the connection mode and the first mixed-metal $[Cu_7GeSe_{13}]$ cluster. *Inorg. Chem. Front.* **2017**, *4*, 387-392.
16. Zhang, Z.; Zhang, J.; Wu, T.; Bu, X.; Feng, P. Three-Dimensional Open Framework Built from Cu-S Icosahedral Clusters and Its Photocatalytic Property. *J. Am. Chem. Soc.* **2008**, *130*, 15238-15239.

17. Behrens, M.; Ordolff, M. E.; Nather, C.; Bensch, W.; Becker, K. D.; Guillot-Deudon, C.; Lafond, A.; Cody, J. A. New three-dimensional thioannates composed of linked Cu_8S_{12} clusters and the first example of a mixed-metal $\text{Cu}_7\text{SnS}_{12}$ cluster. *Inorg. Chem.* **2010**, *49*, 8305-8309.
18. Zhang, R.-C.; Zhang, C.; Ji, S.-H.; Ji, M.; An, Y.-L. Synthesis and characterization of $(\text{H}_2\text{dab})_2\text{Cu}_8\text{Ge}_4\text{S}_{14}\cdot 2\text{H}_2\text{O}$: An expanded framework based on icosahedral Cu_8S_{12} cluster. *J. Solid State Chem.* **2012**, *186*, 94-98.
19. Zhang, R. C.; Yao, H. G.; Ji, S. H.; Liu, M. C.; Ji, M.; An, Y. L. $(\text{H}_2\text{en})_2\text{Cu}_8\text{Sn}_3\text{S}_{12}$: a trigonal Cu_3S_3 -based open-framework sulfide with interesting ion-exchange properties. *Chem. Commun.* **2010**, *46*, 4550-4552.